Mauricio D. Dorfman,[1] Jordan E. Krull,[1] Jarrad M. Scarlett,[1] Stephan J. Guyenet,[1] Mini P. Sajan,[2,3] Vincent Damian,[1] Hong T. Nguyen,[1] Michael Leitges,[4] Gregory J. Morton,[1] Robert V. Farese,[2,3] Michael W. Schwartz,[1] and Joshua P. Thaler[1]

Deletion of Protein Kinase C λ in POMC Neurons Predisposes to Diet-Induced Obesity

Diabetes 2017;66:920–934 | DOI: 10.2337/db16-0482

OBESITY STUDIES

Effectors of the phosphoinositide 3-kinase (PI3K) signal transduction pathway contribute to the hypothalamic regulation of energy and glucose homeostasis in divergent ways. Here we show that central nervous system (CNS) action of the PI3K signaling intermediate atypical protein kinase C (aPKC) constrains food intake, weight gain, and glucose intolerance in both rats and mice. Pharmacological inhibition of CNS aPKC activity acutely increases food intake and worsens glucose tolerance in chow-fed rodents and causes excess weight gain during high-fat diet (HFD) feeding. Similarly, selective deletion of the aPKC isoform *Pkc-λ* in proopiomelanocortin (POMC) neurons disrupts leptin action, reduces melanocortin content in the paraventricular nucleus, and markedly increases susceptibility to obesity, glucose intolerance, and insulin resistance specifically in HFD-fed male mice. These data implicate aPKC as a novel regulator of energy and glucose homeostasis downstream of the leptin-PI3K pathway in POMC neurons.

Energy homeostasis maintains the stability of adipose tissue fuel stores through the coordinated regulation of food intake and energy expenditure (1). This process requires engagement of specialized populations of hypothalamic arcuate nucleus (ARC) neurons including the orexigenic neuropeptide Y (NPY)/agouti-related peptide (AgRP) and anorexigenic proopiomelanocortin (POMC) cells. In response to input from circulating hormones and nutrients reflective of energy availability, ARC neurons modulate downstream circuits that regulate both food consumption and metabolic rate. The melanocortin system, a critical component of this regulatory machinery, involves the opposing actions of the anorexigenic POMC protein by-product α melanocyte-stimulating hormone (α-MSH) and the orexigenic neuropeptide AgRP released into the paraventricular nucleus (PVN) to compete for binding to the melanocortin 4 receptor (MC4R) (1,2). If melanocortin signaling is disrupted, animals (and humans) become hyperphagic and obese, particularly in response to a high-fat diet (HFD) (2). Thus, identifying factors that regulate POMC neuron function is an important step in developing effective obesity therapeutics.

The adipokine leptin also plays a key role in energy homeostasis by defending against body weight gain, in part through coordinately activating POMC neurons and suppressing AgRP neurons (3–5). Upon binding to POMC neurons, leptin activates a number of intracellular signaling networks, including the Jak-Stat3 and phosphoinositide 3-kinase (PI3K) pathways (4,6), ultimately driving increased neuronal activity and melanocortin production. Analysis of POMC neuron–specific transgenic mouse models over the past decade has helped to clarify the roles of these signaling intermediates in leptin action and body weight regulation. While POMC cell–specific deletion of either the leptin receptor (7–9) or Stat3 (10) results in a modest degree of obesity when eating normal chow (as yet untested with an HFD), disruption of the downstream effector PI3K (p110 subunits) (11,12) or its target phosphoinositide-dependent kinase (PDK) (13,14) results in susceptibility to weight gain and diet-induced obesity

[1]UW Diabetes Institute and Department of Medicine, University of Washington, Seattle, WA
[2]Department of Internal Medicine, University of South Florida College of Medicine, Tampa, FL
[3]Research & Internal Medicine Services, James A. Haley VA Medical Center, Tampa, FL
[4]The Biotechnology Centre of Oslo, University of Oslo, Oslo, Norway
Corresponding author: Joshua P. Thaler, jpthaler@uw.edu.

Received 18 April 2016 and accepted 2 January 2017.
This article contains Supplementary Data online at http://diabetes.diabetesjournals.org/lookup/suppl/doi:10.2337/db16-0482/-/DC1.

(DIO), along with defects in glucose regulation. These results suggest that PI3K-mediated signaling in POMC neurons is critical for maintaining metabolic homeostasis and underscore the importance of further investigating the downstream mediators of this pathway.

In peripheral tissues, stimulation of the PI3K pathway results in phosphorylation and activation of PDK and the downstream kinases Akt and protein kinase C (PKC) ζ/λ (collectively termed atypical PKC [aPKC]) (15,16). While Akt has a well-established role in insulin signaling, aPKC has received much less attention because of the early embryonic lethality of deleting PKC-λ (17), the major aPKC isoform in mice, and because of its more complex function in metabolic homeostasis. Thus, whereas muscle-specific PKC-λ knockout (KO) mice show impaired glucose transport in muscle and consequent glucose intolerance and insulin resistance (18), deletion or chemical inhibition of hepatic PKC-λ has the opposite effect (19,20), improving insulin sensitivity and resistance to DIO through reduced de novo lipogenesis and hepatic inflammation. Interestingly, total-body PKC-λ heterozygotes have an incompletely penetrant obesity phenotype and impaired muscle and adipose glucose uptake, yet glucose tolerance remains normal as a result of the salutary effects of reduced hepatic aPKC (21). By contrast, total-body PKC-ζ KOs have normal body weight but increased HFD-induced insulin resistance arising from overproduction of interleukin-6 in adipose tissue (22). Thus, it seems that *1*) PKC-λ is the predominant aPKC associated with body weight regulation; *2*) the two aPKC isoforms are not functionally redundant; and *3*) the effect of aPKC gene deletion depends on the cellular context, as it has simultaneous effects on multiple pathways.

Little is known about the role of aPKC in the central nervous system (CNS), although both isoforms are expressed in many brain regions, including the hypothalamus (23), and aPKC is involved in establishing neuronal polarity during development (24,25). Involvement of CNS aPKC in metabolic regulation has been demonstrated for endotoxin-induced inflammatory anorexia but not acute pharmacological leptin-mediated anorexia (26). Nevertheless, aPKC is highly expressed in hypothalamic neurons, its enzymatic activity is stimulated by CNS administration of leptin, and it can mediate leptin action in vitro (26). Overall, these data suggest that aPKC may contribute to energy and glucose homeostasis regulation downstream of PI3K/PDK in leptin-sensitive neurons. To clarify the contribution of CNS aPKC to energy homeostasis and susceptibility to obesity, we investigated the metabolic consequences of reducing CNS aPKC activity using a specific peptide inhibitor (27) in rats and selectively deleting the PKC-λ isoform in POMC neurons in mice. These complementary methods implicate aPKC activity as a physiological mediator of leptin action and melanocortin content that serves to constrain food intake and limit both HFD-induced weight gain and glucose intolerance.

RESEARCH DESIGN AND METHODS

Animals

Pomc-Cre and *Pkc-λ*$^{loxP/loxP}$ mice (28) on a C57BL/6J background were interbred to generate *Pomc-Cre*$^{+}$*/Pkc-λ*$^{loxP/loxP}$ (POMC-λKO) and *Pomc-Cre*$^{-}$*/Pkc-λ*$^{loxP/loxP}$ (wild-type [WT]) genotypes. Though *Pkc-λ*$^{loxP/loxP}$ mice contain a neomycin resistance gene (*Neo*) incorporated into the intronic region of the *Pkc-λ* gene (Fig. 3*A*), this cassette does not alter expression of *Pkc-λ* mRNA or protein (17,18,29). Hence, *Pomc-Cre*$^{-}$*/Pkc-λ*$^{loxP/loxP}$ are referred to as WT throughout. PCR genotyping was performed on genomic DNA using *Cre* primers and nested primers near *Pkc-λ* exon 2 (see Fig. 2). Separation of genotypes and group housing was required because of the increased sensitivity of POMC-λKO animals to stress-induced behavioral responses to isolation (data not shown). These studies also used male *Pomc-Tau-Gfp* and *ob/ob* mice (The Jackson Laboratory) and male Wistar rats (Harlan/Envigo).

Animals were housed in temperature-controlled rooms with a 12-h light/12-h dark cycle under specific pathogen–free conditions. All procedures were performed in accordance with the *Guide for the Care and Use of Laboratory Animals* from the National Institutes of Health and were approved by the Animal Care Committee at the University of Washington.

Reagents

These studies used leptin (provided by Dr. A. F. Parlow, National Hormone and Peptide Program), insulin (Humulin R; Eli Lilly), and myristoylated aPKC pseudosubstrate inhibitor (INH) (Invitrogen).

Rat Studies

Third ventricle (3V)–cannulated rats (n = 8 or 9/group) received INH (2 nmol in 2 μL) intracerebroventricularly (ICV) or saline vehicle during the light cycle, and chow food intake, energy expenditure, and ambulatory activity over 24 h after injection were measured in metabolic cages (Columbus Instruments), as previously described (30). Separately, the same protocol (n = 6 or 7 mice/group) was followed by a glucose tolerance test (GTT; see below) 4 h after the ICV injection.

For chronic studies, 3V-cannulated rats received INH (6 nmol/day ICV) or saline vehicle infusions for 14 days while fed normal rodent chow. Separately, rats with a cannula placed in the lateral ventricle (LV) received INH (6 nmol/day ICV) or saline vehicle infusions for 14 days while fed an HFD (60% kcal from fat, D12492; Research Diets) beginning on day 2 after surgery. Body weight and food intake were measured daily in both studies.

Surgery

For acute pharmacological studies, rats were implanted with a cannula (Plastics One) directed to the 3V using standard stereotaxic coordinates (2.2 mm posterior to bregma; 0.0 mm lateral to the sagittal suture, and 7.7 mm below the skull surface). For chronic infusions, rats were implanted with a 3V or LV cannula (0.8 mm posterior to

bregma; 1.5 mm lateral to the sagittal suture, and 3.6 mm below the skull surface) connected to a subcutaneous osmotic minipump (DURECT Corp) for ICV infusions over 14 days.

Mouse Studies

Eight-week-old male and female POMC-λKO and WT mice (n = 5–10/group) received 7 weeks of chow or an HFD; food intake and body weight were monitored weekly. Body composition was analyzed in all mice using quantitative magnetic resonance spectroscopy (EchoMRI 3-in-1) (31) at the beginning and end of the HFD feeding period. Given the requirement for group housing to avoid isolation stress, calorimetry was not performed in POMC-λKO mice.

A separate cohort of male and female POMC-λKO and WT mice (n = 5–9/group) was subjected to 1 week of HFD feeding for analysis of glucose homeostasis before body weight divergence between genotypes. All four groups underwent a GTT and insulin tolerance test (ITT), as described below.

aPKC expression in POMC neurons was analyzed in male *Pomc-Tau-Gfp* mice fed chow or an HFD for 5 months. At the end of the study, hypothalamic tissue was collected for immunohistochemical (IHC) studies (n = 5/group) or Western blotting (n = 8/group).

To assess the responsiveness to leptin of POMC neurons that express aPKC, *Pomc-Tau-Gfp* mice were injected with leptin (5 μg/g body weight i.p.) and perfused 1 h later for aPKC and phospho-STAT3 (p-STAT3) IHC analysis (described below).

To determine the effect of leptin on aPKC activity, adult male *ob/ob* mice (n = 6/group) were subcutaneously implanted with an osmotic minipump (Alzet) containing either vehicle (PBS, pH 7.9) or leptin (100 ng/h). To allow for recovery after surgery, both groups received a vehicle run-in for the first 24 h of the infusion. Approximately 6 h into the leptin infusion period, a blood sample was taken from the tail vein to verify physiological leptin replacement (data not shown). To avoid the confounding effect of suppression of food intake by leptin, all animals were fasted overnight before postmortem collection of hypothalamic tissue.

Glucose and Insulin Tolerance Testing

GTTs were conducted using a glucose bolus (30% D-glucose; 2 g/kg i.p.) administered to mice or rats fasted for 5 h. ITTs were conducted using regular insulin injections (0.75 IU/kg i.p.) into nonfasted mice. For both GTTs and ITTs, glucose levels were measured in tail capillary blood using a glucometer (OneTouch Ultra).

Leptin Sensitivity

Weight-matched male mice (eight WT and eight POMC-λKO mice) fed a chow diet received daily injections of saline (200 μL/day i.p.) for 2 days, followed by daily leptin (2 μg/g body weight i.p.) for 2 days; body weight and food intake were measured daily. At the end of the study, mice (n = 4/group) received saline or leptin (2 μg/g body weight i.p.) and were perfused 90 min later for c-Fos IHC analysis.

Blood Collection and Tissue Processing

Upon completion of the study, plasma leptin levels were determined in postmortem blood samples using ELISA (Crystal Chem). For IHC studies, anesthetized animals were perfused with PBS, followed by 4% paraformaldehyde in PBS. Brains were removed, postfixed in 4% paraformaldehyde, protected with sucrose (25%), and cryosectioned (14-μm slices in the coronal plane through the hypothalamus), then mounted on slides and stored at −80°C for IHC staining. For Western blotting and aPKC activity, hypothalamic blocks were dissected and stored at −80°C until protein extraction.

IHC Staining

Anatomically matched hypothalamic sections from *Pomc-Tau-Gfp* mice were treated with goat anti–green fluorescent protein (1:10,000; Fitzgerald Industries), rabbit anti-PKC-ζ/λ (1:1,000; Santa Cruz Biochemicals), or rabbit anti-p-STAT3 (1:1,000; Sigma). For p-STAT3 immunostaining, the sections required pretreatment for 15 minutes with 1% NaOH. Separately, sections from WT and KO mice were incubated with rabbit anti-c-Fos (1:100,000; Oncogene Science, Inc.) or goat anti-α-MSH (1:10,000; Millipore). After primary incubation overnight at 4°C, all slides were processed with appropriate fluorescent secondary antibodies (Alexa Fluor 488 and 594; 1:1,000; Life Technologies). Stained sections were imaged using a cooled charge-coupled device camera attached to a DS-Ri1 epifluorescence microscope (Nikon, Tokyo, Japan). Cell number and colocalization were determined in a blinded fashion (n = 4 sections from three mice/group).

Western Blotting

Hypothalamic tissue was homogenized in 500 μL of lysis buffer (T-PER; Thermo Fisher Scientific, Rockford, IL) containing protease inhibitor cocktail (cOmplete; Sigma Aldrich, St. Louis, MO) and phosphatase inhibitors (PhosSTOP Phosphatase Inhibitor Cocktail Tablets; Roche, Indianapolis, IN). After proteins were resolved using SDS-PAGE and transferred to nitrocellulose membranes, immunoblotting was performed with rabbit anti-PKC-ζ/λ antibody (1:1,000; Santa Cruz Biochemicals), followed by horseradish peroxidase–conjugated donkey antirabbit antibody (1:5,000; Cell Signaling Technology, Danvers, MA), and visualized with an enhanced chemiluminescent substrate (Thermo Fisher Scientific). Membranes were subsequently stripped and reprobed with rabbit anti-phospho-PKC-ζ/λ antibody (1:1,000; Cell Signaling Technology). Images were quantified by densitometry using ImageJ software (National Institutes of Health) with phosphorylated aPKC normalized to total aPKC levels.

aPKC Activity

aPKC activity was measured as described previously (15,16), using total aPKC isolated from hypothalamic lysates by immunoprecipitation with rabbit anti-PKC-ζ/λ polyclonal antiserum (Santa Cruz Biotechnology). Immunoprecipitated aPKCs were collected on Sepharose-AG

beads. Isolated aPKCs were incubated for 8 min at 30°C in 100 μL of buffer containing 50 mmol/L Tris-HCl (pH 7.5), 100 μmol/L Na_3VO_4, 100 μmol/L $Na_4P_2O_7$, 1 mmol/L NaF, 100 μmol/L phenylmethylsulfonyl fluoride, 4 μg phosphatidylserine (Sigma), 50 μmol/L [γ-^{32}P]ATP (NEN/Life Science Products, Waltham, MA), 5 mmol/L $MgCl_2$, and, as a substrate, 40 μmol/L serine analog of the PKC-ε pseudosubstrate (Enzo Life Sciences, Farmingdale, NY). After incubation, ^{32}P-labeled substrate was trapped on P-81 filter paper and counted in a liquid scintillation counter.

Real-Time PCR

Total RNA was extracted using an RNeasy Mini Kit according to the manufacturer's instructions (Qiagen), and reverse-transcribed with avian myeloblastosis virus reverse transcriptase (Promega, Fitchburg, WI). Levels of mRNA for *Pomc*, *Pcsk1*, *Pcsk2*, *Cpe*, *Pam*, and *18S* RNA (internal control) were measured using semiquantitative real-time PCR on an ABI Prism 7900HT system (Applied Biosystems). The primer sequences were as follows: *Pomc* forward: 5′-CGCTCCTACTCCATGGAGCACTT-3′, reverse: 5′-TCGCCTTCCAGCTCCCTCTTG-3′; *Pcsk1* forward: 5′-CAATGTGGAATCAGCAGTGGT-3′, reverse: 5′-TCCACTC CAAGCCATCATCC-3′; *Pcsk2* forward: 5′-GACTTCAGCAG CAATGACCC-3′, reverse: 5′-CTCCTGCACACCTAGTTCC A-3′; *Cpe* forward: 5′-CCGGTGGAATGCAAGACTTC-3′, reverse: 5′-CCAGGTAGCTGATGAGGGAG-3′; *Pam* forward: 5′-ATGCTGCTGTTTGGATGCAA-3′, reverse: 5′-TGGCTT TATCTGTACAGGTTCCT-3′.

In Situ Hybridization

Pomc mRNA and *Pkc-λ* or *Pkc-ζ* mRNA in the brains of POMC-λKO and WT mice were visualized simultaneously, as previously reported (32). Coronal sections (20 μm thick) were collected in a 1:4 series through the hypothalamus, from the diagonal band of Broca caudally through the mammillary bodies (bregma –5.00 mm). Antisense ^{33}P-labeled Pkc-λ riboprobe (corresponding to bases 2382–2822 of mouse Pkc-λ; GenBank accession no. NM_008857.3), or Pkc-ζ riboprobe (corresponding to bases 1995–2319 of mouse Pkc-ζ; GenBank accession no. NM_008860.3), and antisense digoxigenin-labeled murine Pomc riboprobe (925 bp; a gift from Dr. Robert Steiner) were denatured, dissolved in hybridization buffer along with transfer RNA (1.7 mg/mL), and applied to slides. Controls used to establish the specificity of Pkc-λ and Pkc-ζ riboprobes included slides incubated with an equivalent concentration of radiolabeled sense Pkc-λ or Pkc-ζ riboprobe, or radiolabeled antisense probe in the presence of excess (1,000×) unlabeled antisense probe. Slides were covered with glass coverslips, placed in a humid chamber, and incubated overnight at 55°C. The following day, slides were treated with RNase A and washed under conditions of increasing stringency. The sections were incubated in blocking buffer and then in Tris buffer containing anti-digoxigenin fragments conjugated to alkaline phosphatase (1:250; Roche Molecular Biochemicals) for 3 h at room temperature. POMC neurons were visualized with Vector Red substrate (SK-5100; Vector Laboratories), according to the manufacturer's protocol. Slides were dipped in 100% ethanol, air dried, and then dipped in NTB liquid emulsion (Carestream Health Co). Slides were developed 9 days (Pkc-ζ) and 11 days (Pkc-λ) later and coverslipped. Cells expressing both Pkc-λ or Pkc-ζ mRNA and Pomc mRNA were identified using previously described criteria (32). Using ImageJ software, we quantified the ratio of the PKC-λ signal in POMC neurons to the background signal in the proximity of each cell. Signal-to-background ratio (SBR) distributions for individual animals were then averaged across the groups to generate a cumulative frequency curve (means and SEMs for each SBR).

Statistical Analyses

All results are presented as mean ± SEM. Statistical analysis using Prism software (GraphPad Software Inc.) involved unpaired two-tailed Student *t* tests, two-way ANOVA with post hoc Tukey testing, or linear regression. *P* values <0.05 were considered statistically significant.

RESULTS

Acute Inhibition of CNS aPKC Activity Increases Food Intake and Glucose Intolerance

We previously showed that CNS aPKC activity *1*) increases with ICV administration of leptin or insulin, and *2*) is a critical mediator of endotoxin-mediated anorexia and fever (26). However, a role for central aPKC in the physiological regulation of energy and glucose homeostasis remained untested. To assess this possibility, we used a cell-permeable myristoylated aPKC pseudosubstrate inhibitor (INH) that acutely reduces aPKC activity with high specificity (27). ICV injection of INH into rats during the light cycle increased food intake at 4 h (2.1 ± 0.4 vs. 3.7 ± 0.3 g) (Fig. 1*A*), with a compensatory elevation of metabolic rate (Supplementary Fig. 1*A* and *B*). Though the effect on energy expenditure was relatively transient, increased intake was still apparent 8 h after injection (at onset of the dark cycle) ($P = 0.10$) (Fig. 1*B*), but was completely absent at 24 h ($P = 0.53$) (Fig. 1*C*). Finally, energy expenditure during the dark cycle (starting 8 h after ICV injection) and ambulatory activity throughout the 24 h period were unaffected by the INH treatment (Supplementary Fig. 1*C*; data not shown).

We next examined the effect of acute central aPKC inhibition on glucose homeostasis by performing a GTT 4 h after ICV administration of either INH or vehicle. In both rats (Fig. 1*D* and *E*) and mice (Supplementary Fig. 2*A* and *B*), INH treatment caused a mild but consistent impairment of glucose tolerance. Together, these data suggest that tonic CNS aPKC activity contributes to the regulation of food intake and glucose homeostasis.

Chronic Inactivation of CNS aPKC Activity Increases Body Weight and Food Intake During HFD Feeding

Given the impact of acute CNS aPKC inhibition on energy homeostasis parameters, we hypothesized that susceptibility to DIO would be increased by chronic inhibition

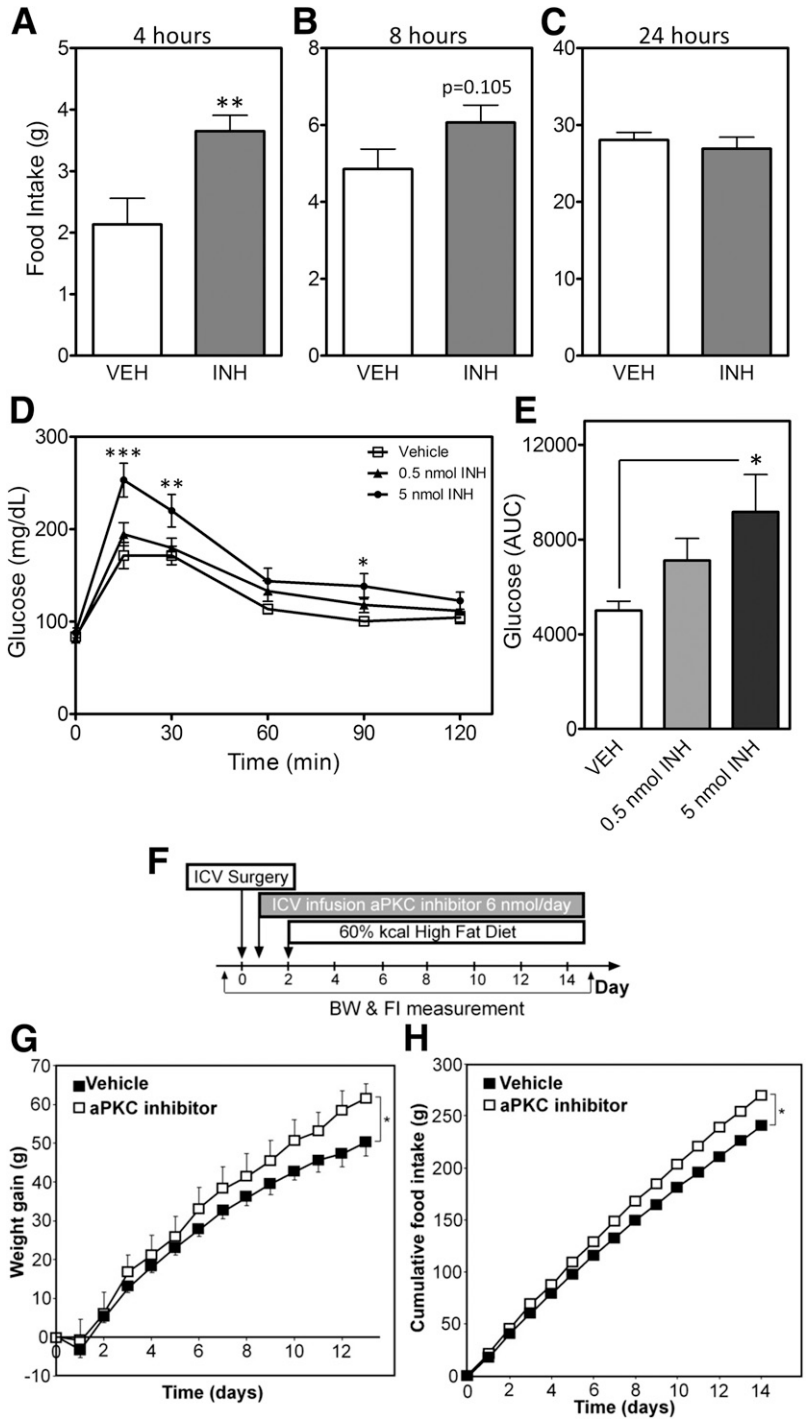

Figure 1—Central administration of the aPKC inhibitor increases body weight (BW), food intake (FI), and glucose intolerance. *A–C*: FI in chow-fed rats measured 4 (*A*), 8 (*B*), and 24 h (*C*) after ICV (3V) injection of an aPKC inhibitor (INH; 0.5 nmol) or vehicle (VEH). In panels *A–C*, data are presented as the mean ± SEM of at least eight animals per group. *D*: Intraperitoneal GTT (2 g/kg) in chow-fed rats 4 h after ICV injection of VEH, 0.5 nmol INH, or 5 nmol INH. *E*: Glucose area under the curve (AUC) analysis of data from panel *D*. In panels *D* and *E*, data are presented as the mean ± SEM of at least six animals per group. *F*: On day 0, Wistar rats were implanted with ICV LV cannulae connected to subcutaneous osmotic mini pumps containing INH (6 nmol/day) or VEH. All rats were switched to an HFD on day 2. Weight gain (*G*) and cumulative FI (*H*) for the 14-day infusions in the VEH and aPKC inhibitor groups. *F–H*: Data are presented as the mean ± SEM of eight rats per group. $^{*}P < 0.05$; $^{**}P < 0.01$; $^{***}P < 0.001$.

of central aPKC activity. To test this hypothesis, we determined the effect of continuous ICV infusion of either INH (6 nmol/day) or saline vehicle for 14 days in adult male Wistar rats fed either an HFD or chow (Fig. 1*F*). As with acute aPKC inhibition, chronic silencing of aPKC activity in the CNS increased food intake without affecting

body weight in chow-fed animals (data not shown). By contrast, central aPKC inhibition in HFD-fed rats increased both weight gain (Fig. 1*G*) and food intake (Fig. 1*H*). Together, these results suggest that CNS aPKC activity serves to constrain food consumption and protect against pathological weight gain.

Atypical PKC Expression in POMC Neurons Increases With HFD Feeding

The infusion studies described above demonstrated that the contribution of CNS aPKC activity to energy homeostasis regulation differs under chow and HFD conditions. To investigate a possible mechanism to explain this diet specificity, we analyzed the impact of HFD feeding on hypothalamic aPKC expression. While overall hypothalamic aPKC expression and activity were unchanged by exposure to an HFD (Fig. 2*H*), IHC analysis of *Pomc-Tau-Gfp* marker mice revealed nearly twice as many aPKC-positive hypothalamic POMC neurons during HFD feeding compared with chow (38% vs. 20%) (Fig. 2*A* and *G*). These data suggest that hypothalamic POMC neurons may be targets for the action of aPKC to constrain diet-induced weight gain.

Generation and Validation of Mice Lacking the *Pkc-λ* Gene in POMC Neurons

Given that aPKC expression increases in ARC POMC neurons during HFD feeding (Fig. 2) and central aPKC inhibition induces metabolic alterations (Fig. 1) reminiscent of phenotypes associated with POMC cell–specific leptin signaling pathway mutants (7–9,11–14), we next investigated the effect of POMC neuron–specific deletion of aPKC on energy homeostasis. Since whole-body *Pkc-ζ* KO mice show no alterations in energy balance or sensitivity to DIO (22), we focused on the PKC-λ isoform of aPKC. To generate animals with a POMC neuron–specific deletion of the *Pkc-λ* gene, we crossed *Pkc-λ*$^{loxP/loxP}$ mice (28) with mice expressing Cre recombinase under the control of the *Pomc* promoter (*Pomc-Cre*$^{+}$) (POMC-λKO) (Fig. 3*A*). PCR amplification of genomic DNA extracted from the hypothalamus, cortex, liver, and muscle (Fig. 3*B*) generated the ~200-bp Cre deletion fragment product only in hypothalamic DNA samples, indicating tissue-specific excision of the loxP-flanked *Pkc-λ* gene. In addition, in situ hybridization analysis revealed lower *Pkc-λ* expression in POMC neurons of POMC-λKO mice than in WT controls (Fig. 3*C*–*E*) with no compensatory change of *Pkc-ζ* mRNA expression (data not shown). Finally, equal numbers of hypothalamic POMC neurons were present in adult POMC-λKO and WT mice (Fig. 3*F*), confirming that deletion of *Pkc-λ* during embryogenesis (earliest activity of the *Pomc* promoter) did not affect general POMC neuron development or cellular survival in adulthood (an important consideration given the role of aPKC in establishing neuronal polarity [25]).

Deletion of *Pkc-λ* in POMC Neurons Predisposes Male Mice to DIO

To assess the effect of POMC neuron–specific *Pkc-λ* deficiency on energy homeostasis, we monitored body weight, body composition, and food intake in male and female mice fed either an HFD or regular chow for 7 weeks. While the body weights of male WT and POMC-λKO mice did not differ on chow, male POMC-λKO mice fed an HFD showed accelerated weight gain, diverging from WT controls within 2 weeks of HFD initiation (Fig. 4*A*). By contrast, female POMC-λKO and WT mice were indistinguishable in all aspects of their metabolic phenotype irrespective of diet (Fig. 4*B*; data not shown). After 7 weeks of HFD feeding, male POMC-λKO mice also had increased fat mass gain relative to WT controls, but no differences in lean mass (Fig. 4*C* and *D*). This effect was attributed to consistently elevated HFD intake among the POMC-λKO mice (Fig. 4*E* and *F*). Notably, the hyperphagia of the POMC-λKO mice relative to WT controls began within the first week of HFD feeding, before body weight separation between the genotypes (data not shown). Thus, male POMC-λKO mice show increased susceptibility to DIO through increased HFD intake.

In some mouse models involving POMC Cre-mediated gene deletion, alterations in the function of pituitary corticotrophs (which also express POMC) can also affect the metabolic phenotype (13,14). To address this possibility, we assessed corticosterone and ACTH levels in male POMC-λKO and WT mice fed chow or an HFD (Supplementary Fig. 3). In contrast to male WT mice, in which HFD feeding doubled serum corticosterone (Supplementary Fig. *3A*) with a compensatory reduction in ACTH (Supplementary Fig. *3B*), male POMC-λKO mice under both diet conditions showed equally elevated corticosterone (Supplementary Fig. *3A*) and lower ACTH levels (Supplementary Fig. *3B*). Similarly, female POMC-λKO mice had elevated corticosterone levels (Supplementary Fig. *3C*). Thus, POMC-λKO mice show diet-independent activation of the hypothalamic-pituitary-adrenal axis in both sexes, but an altered metabolic phenotype in only HFD-fed males. Therefore, excessive corticosterone production is an implausible driver of susceptibility to obesity in male POMC-λKO mice but more likely reflects the overall sensitivity to stress of the POMC-λKO strain (see RESEARCH DESIGN AND METHODS).

Pkc-λ Deficiency in POMC Neurons Alters Glucose Homeostasis

To evaluate the effects of *Pkc-λ* deficiency in POMC neurons on peripheral glucose homeostasis, we performed both an intraperitoneal GTT and an ITT in male POMC-λKO mice and WT controls. While the 7-week period of HFD feeding induced only moderate glucose intolerance in WT mice (Fig. 5*A* and *B*), POMC-λKO mice showed markedly elevated basal glucose levels (Fig. 5*A*, time point = 0 min), impaired glucose tolerance (Fig. 5*A* and *B*), and increased insulin resistance (Fig. 5*C*). Insulin secretion remained intact, however, with large elevations in both fasting and glucose-stimulated insulin levels in POMC-λKO mice relative to WT controls (Fig. 5*D* and *E*).

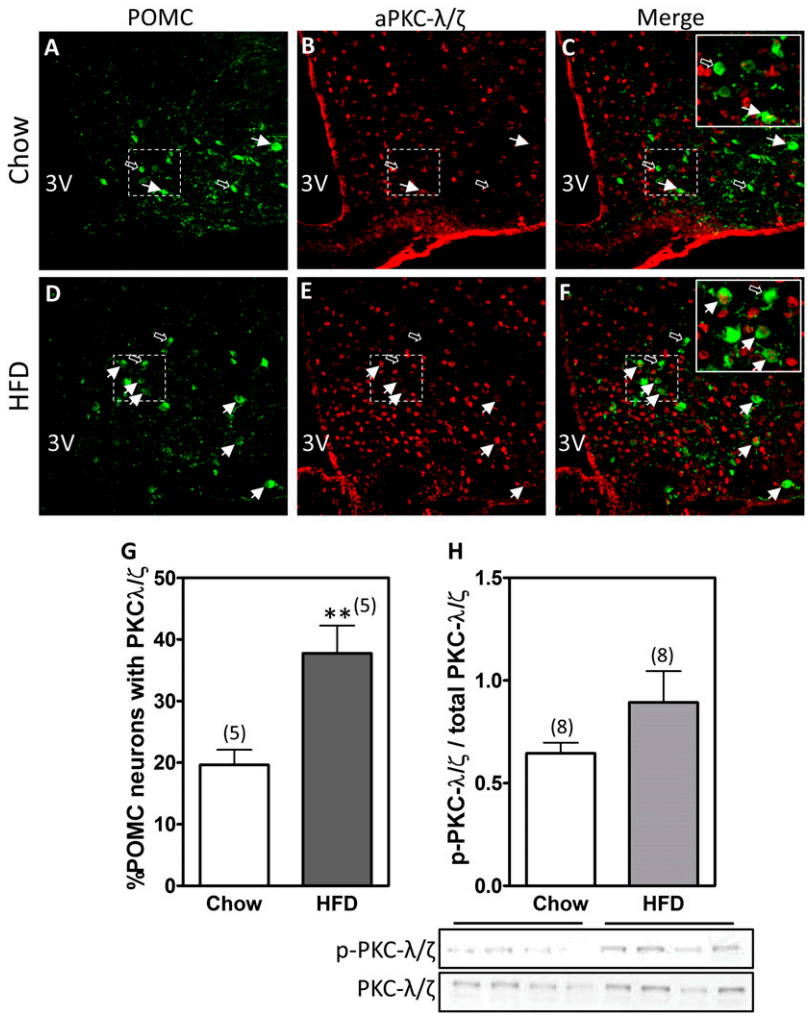

Figure 2—aPKC expression increases within POMC neurons in HFD-fed mice. PKC-λ/ζ was detected via immunofluorescence in hypothalamic sections from *Pomc-tau-Gfp* mice fed chow or an HFD for 4 months. *A* and *D*: Representative unstained images showing green fluorescent protein (GFP) expression in POMC neurons from mice fed chow (*A*) or an HFD (*D*). *B* and *E*: The same sections from *A* and *D* were incubated with an antibody that recognizes both the λ and ζ PKC isoforms. *C* and *F*: Merged images revealing POMC neurons that express PKC-λ/ζ (yellow cells). White arrows indicate double-positive cells, whereas black arrows demonstrate PKC-λ/ζ-negative POMC neurons. *G*: Double-positive cells (GFP and PKC-λ/ζ) were quantified in a total of four brain sections from five animals in each group. Bars represent the mean percentage ± SEM of POMC cells expressing PKC-λ/ζ. *H*: Immunoblot of phosphorylated aPKC (p-PKC-λ/ζ) and total aPKC (PKC-λ/ζ) in hypothalamic homogenates. Bars represent the ratio of mean pixel densities ± SEM between p-PKC-λ/ζ and total PKC-λ/ζ bands quantified from eight samples per group. $^{**}P < 0.01$.

As expected, there were no differences in glucose homeostasis parameters between the chow-fed groups of WT and POMC-λKO mice (Fig. 5*A* and *C*).

To assess whether the glucose intolerance and insulin resistance observed in POMC-λKO mice was independent of body weight gain, a GTT and ITT were performed in male mice after 1 week on an HFD (Supplementary Fig. 4*A*), before body weights diverge significantly between genotypes (Fig. 4*A*). Compared with WT mice, male POMC-λKO mice showed a small, statistically significant increase in glucose levels during the first 30 min of the GTT (Supplementary Fig. 4*A*) and ITT (Supplementary Fig. 4*C*), but no difference in glucose area under the curve (Supplementary Fig. 4*B*). As an additional approach to test the direct effect of PKC-λ action in POMC neurons on glucose homeostasis, we examined female POMC-λKO mice fed an HFD, as they did not differ from WT controls in terms of body weight or food intake (Fig. 4*B*; data not shown). In contrast with the findings in males, glucose tolerance was indistinguishable between female WT and POMC-λKO mice after 1 and 7 weeks of HFD feeding (Supplementary Fig. 4*D* and *E*; data not shown). Together, these findings suggest that during HFD feeding, PKC-λ signaling in POMC neurons is required for normal glucose tolerance in male mice but not females. Though the underlying mechanism seems to be partially independent of weight, the combined effect of diet and obesity results in severely impaired glucose homeostasis.

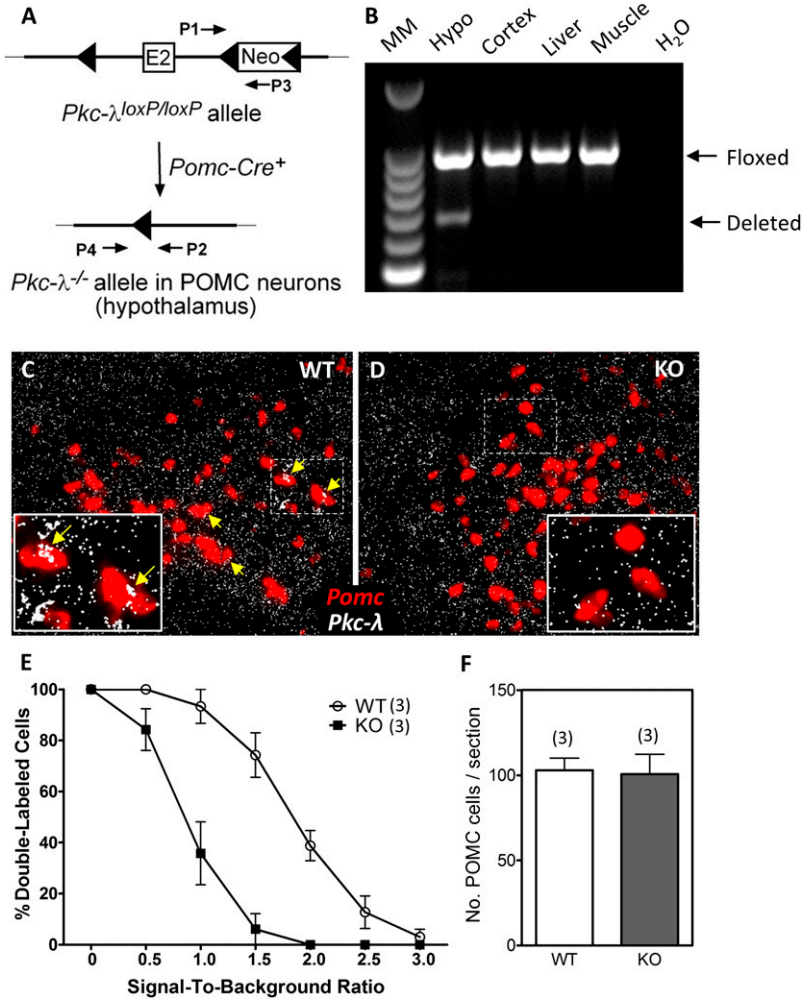

Figure 3—Validation of mice lacking the *Pkc-λ* gene in POMC neurons. *A*: Schematic of the genomic DNA region around exon 2 of *Pkc-λ* in mice carrying a targeted *Pkc-λ* allele (*Pkc-λ*$^{loxP/loxP}$). The PCR primers P1 and P3 amplify an intronic region located downstream of *Pkc-λ* exon 2 (E2) that contains a loxP-flanked Neo cassette insert. After Cre-mediated excision of exon 2 and the Neo cassette, a PCR amplification product identifying the deleted *Pkc-λ* allele (*Pkc-λ*$^{-/-}$) becomes detectable using primers P2 and P4. *B*: PCR amplification products from genomic DNA using primers P1–P3 (Floxed) and P2–P4 (Deleted). Tissues were dissected from a POMC-λKO mouse. Lanes represent (from left to right) a 100-bp DNA molecular marker (MM) ladder, hypothalamus (Hypo; positive for recombination), cortex, liver, muscle, H_2O control. *C* and *D*: In situ hybridization on brain sections from WT (*C*) and POMC-λKO (*D*) animals using probes against *Pomc* (red) and *Pkc-λ* (white) mRNA. The dashed rectangles denote regions corresponding to magnified insets. Yellow arrows indicate POMC neurons that express *Pkc-λ*. *E*: Percentage of cells coexpressing *Pomc* and *Pkc-λ* mRNA as a function of SBR. The ordinate value represents the percentage of cells having an SBR greater than the value of the abscissa. Data are mean ± SEM from three animals per group. *F*: Quantification of arcuate POMC neurons in WT and POMC-λKO mice. Positive cells quantified on six sections from three animals per group. Bars represent the mean ± SEM.

aPKC Is a Mediator of Leptin Action in POMC Neurons

The ability of CNS aPKC signaling to limit food intake and protect against DIO raises the possibility that this enzyme mediates intracellular responses to leptin and hence is required for intact leptin sensitivity. This hypothesis is consistent with our previous demonstration of increased hypothalamic aPKC activity following ICV administration of leptin in rats (26). Similarly, in leptin-deficient *ob/ob* mice, hypothalamic aPKC activity increased by ~50% following physiological leptin replacement (Supplementary Fig. 5). Finally, aPKC is expressed in the leptin-responsive subset of POMC neurons, as demonstrated by colocalization of aPKC with immunoreactivity for p-STAT3 in response to intraperitoneal leptin administration (Supplementary Fig. 6). These observations, together with the similar phenotypes of the POMC-λKO and other POMC-specific mouse models lacking leptin signaling intermediates downstream of PI3K (11–14), suggested that the metabolic abnormalities of POMC-λKO mice might arise from reduced hypothalamic leptin action. To test this hypothesis, we measured leptin sensitivity in weight-matched, chow-fed male POMC-λKO and WT mice to avoid confounding from differences in food intake and body weight during HFD feeding. Once-daily injection with leptin (2 μg/g i.p.) for 2 consecutive days significantly reduced body weight (Fig. 6*A*) and food intake

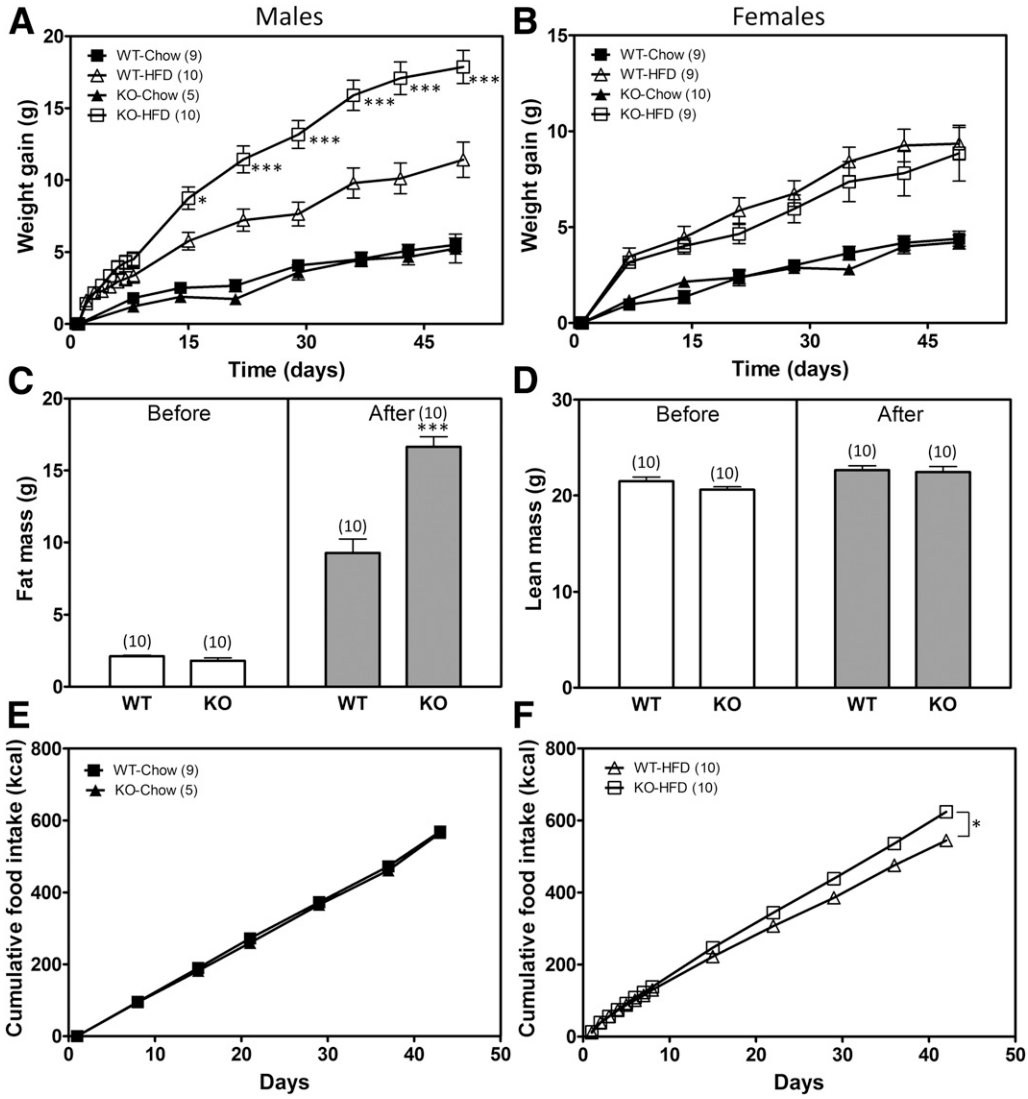

Figure 4—Predisposition toward DIO in POMC-λKO mice. *A* and *B*: Average weight gain in WT and POMC-λKO male (*A*) and female (*B*) mice on normal chow diet and an HFD. Animals on an HFD were weighed daily during the first week. $^{*}P < 0.05$ and $^{***}P < 0.001$ vs. WT mice on an HFD. *C*: Fat mass in WT and POMC-λKO male mice before (left panel) and after (right panel) 7 weeks of HFD. $^{***}P < 0.001$. *D*: Lean mass in WT and POMC-λKO male mice before (left panel) and after (right panel) 7 weeks of HFD. *E*: Cumulative food intake (kilocalories) in WT and POMC-λKO male mice fed chow for 7 weeks. *F*: Cumulative food intake (kilocalories) in WT and POMC-λKO male mice fed an HFD for 7 weeks. $^{*}P < 0.05$. Data are mean ± SEM from 5–10 animals per group.

(Fig. 6*B*) in WT but not POMC-λKO mice, indicating that PKC-λ is necessary for the anorexic action of leptin mediated by POMC neurons. As further evidence of leptin resistance, plasma leptin levels were elevated in POMC-λKO mice relative to WT controls, even when body weights were not different (Fig. 6*C*). Finally, to determine whether PKC-λ is required for leptin-mediated neuronal activation, we used IHC to detect c-Fos induced by leptin in POMC-λKO and WT mice (since aPKC is not involved in the leptin receptor–Jak-Stat pathway). At baseline, c-Fos expression in the arcuate nucleus of the hypothalamus did not differ between vehicle-injected WT and POMC-λKO mice (Fig. 6*D*, *F*, and *H*). By contrast, administration of leptin (2 μg/g i.p.) caused a marked increase of c-Fos-positive neurons in the ARC of WT but not POMC-λKO animals (compare Fig. 6*E* and *G*; quantification in Fig. 6*H*), suggesting a profound reduction in hypothalamic leptin action.

To address the potential mechanism by which aPKC-mediated leptin resistance promotes hyperphagia and weight gain, we investigated the melanocortin pathway. Within POMC neurons, a series of enzymes including prohormone convertases PCSK1 and PCSK2, carboxypeptidase E, and peptidylglycine α-amidating monooxygenase (PAM) sequentially process the POMC polypeptide to produce α-MSH, a potent anorexigenic neuropeptide that acts on MC4R in the PVN (33). Because leptin increases the expression of *Pomc* and its processing enzymes (33), we postulated that this function would be impaired in POMC-λKO mice. Contrary to our hypothesis, *Pomc*

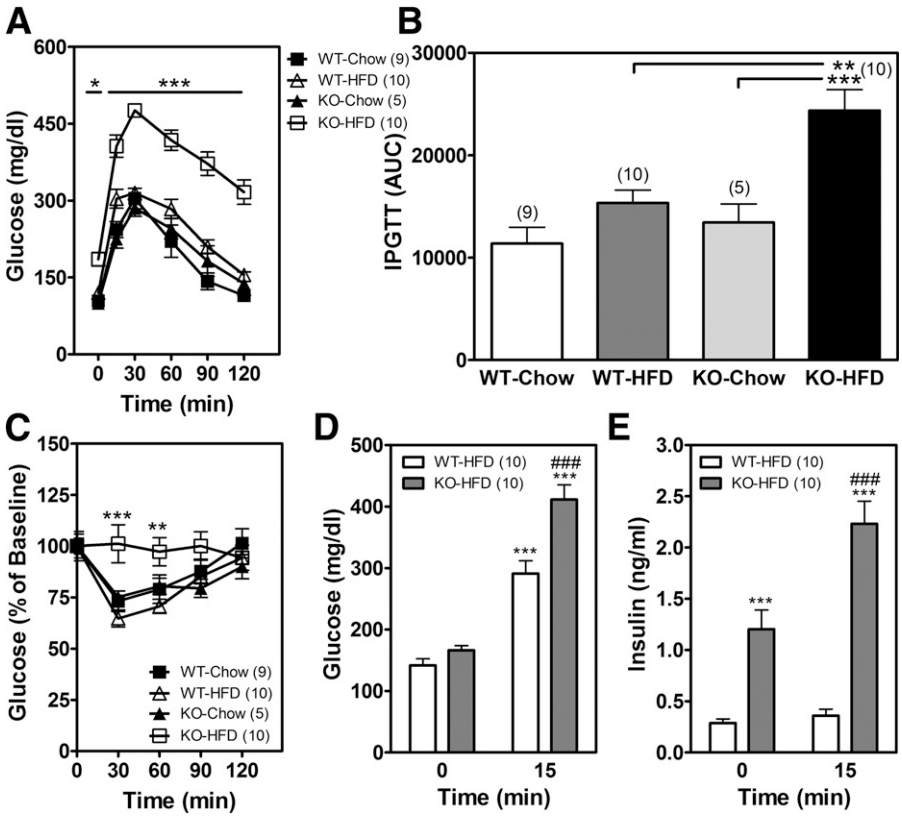

Figure 5—Glucose and insulin intolerance in POMC-λKO mice. *A*: GTT (2 g/kg) in male WT and POMC-λKO mice after 7 weeks on chow or an HFD. $^{*}P < 0.05$ and $^{***}P < 0.001$ compared with WT mice fed an HFD. *B*: Area under the curve (AUC) analysis of *A*. IPGTT, intraperitoneal glucose tolerance test. $^{**}P < 0.01$ and $^{***}P < 0.001$ compared with WT mice fed an HFD and KO mice fed a chow diet, respectively. *C*: ITT (0.75 units/kg) in male WT and POMC-λKO mice after 7 weeks on chow or an HFD. Data are presented as a percentage of baseline. $^{**}P < 0.01$ and $^{***}P < 0.001$ compared with WT mice fed an HFD. *D* and *E*: Blood glucose (*D*) and blood insulin (*E*) levels 0 min and 15 min after glucose administration (2 g/kg i.p.) in WT and POMC-λKO males after 7 weeks on chow or an HFD. $^{***}P < 0.001$ compared with time 0 min; $^{###}P < 0.001$ compared with WT mice fed an HFD at time 15 min. Data are mean ± SEM from 5–10 animals per group.

mRNA levels were increased in POMC-λKO mice compared with WT controls, whereas the expression of *Pcsk1*, *Pcsk2*, and *Cpe* was unchanged (Fig. 6*I*). *Pam* expression was substantially reduced (Fig. 6*I*), however, raising the possibility of altered α-MSH availability in the POMC-λKO mice. Indeed, immunostaining of α-MSH in the PVN revealed an ~30% decrease in α-MSH immunoreactivity (Fig. 6*J–L*). Together, these data suggest that aPKC deletion from POMC neurons promotes leptin resistance and reduced melanocortin content to induce hyperphagia and increase susceptibility to DIO.

DISCUSSION

Effector molecules common to multiple signaling pathways play distinct roles in critical neuronal cell types involved in energy homeostasis regulation. In this study, we show that aPKC is a critical downstream kinase in the leptin signaling pathway; food intake, glucose intolerance, and HFD-induced body weight gain were increased by CNS aPKC inhibition. Moreover, aPKC expression doubles in POMC neurons during HFD feeding, and deletion of the *Pkc-λ* aPKC isoform from these cells reduces melanocortin content and causes central leptin resistance along with increased susceptibility to DIO and glucose intolerance in male mice. Thus, PKC-λ is an important signaling intermediate in POMC neurons that protects against metabolic derangements induced by HFD feeding.

Though both leptin and insulin can signal through PI3K, the early view that they act additively in POMC neurons to control energy and glucose homeostasis (1,6) has been challenged by more recent results. Insulin and leptin seem to signal in nonoverlapping and possibly competing subsets of POMC neurons (34). Hence, the combined deficiency of insulin and leptin receptors in POMC neurons reduced—rather than increased—the propensity toward weight gain compared with deletion of the leptin receptor alone (35,36). By contrast, alterations in the function of downstream signaling intermediates (Jak-Stat, PI3K-PDK, AMPK) in POMC neurons show more consistent and severe metabolic dysregulation. In particular, POMC neuron–specific deletion of either the PDK1 or p110 components of the PI3K pathway results in hyperphagic mice with enhanced susceptibility to DIO (11–14). Similarly, we demonstrated that deficiency of PKC-λ, a PI3K-PDK target, causes severe systemic insulin resistance with HFD-induced obesity. Together, these

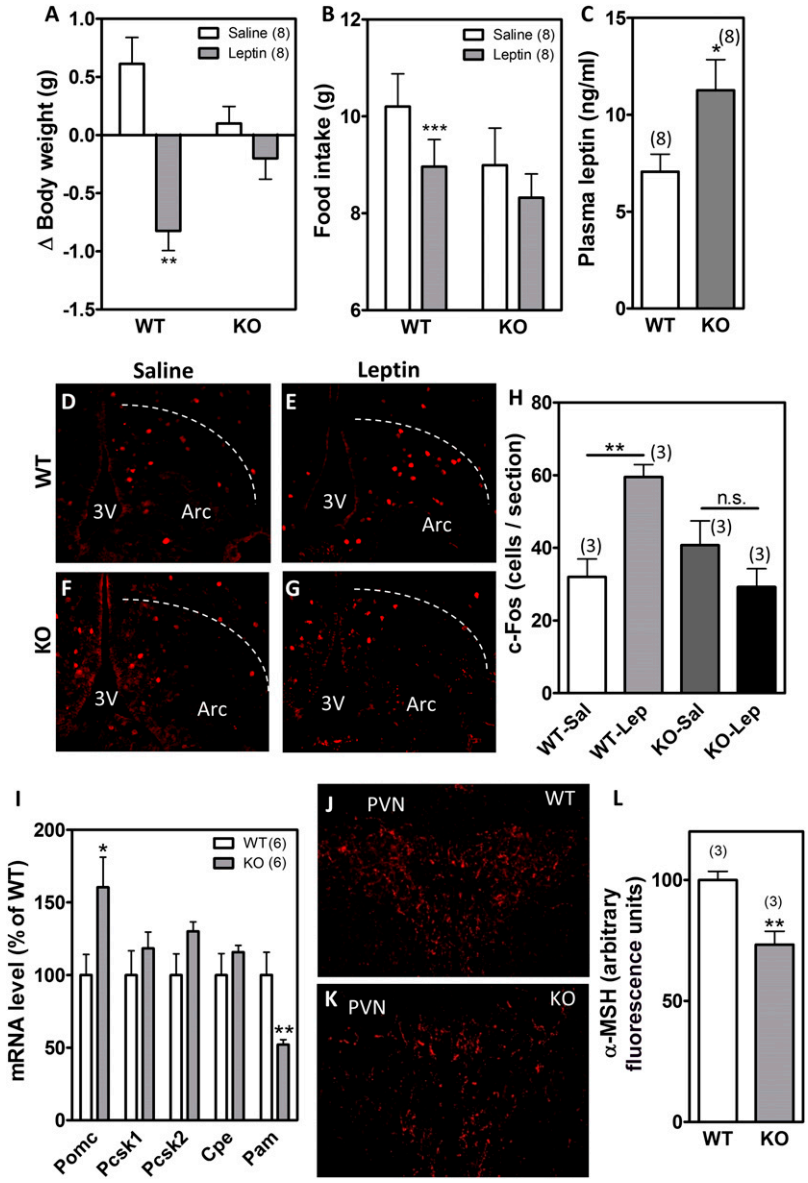

Figure 6—POMC-λKO mice are less responsive to leptin. Body weight change (*A*) and 48-h food intake (*B*) after saline or leptin injections (2 μg/g/day i.p.) in WT and POMC-λKO mice. *C*: Plasma leptin levels in WT and POMC-λKO mice. *D–G*: Representative images showing c-Fos expression in the ARC 30 min after intraperitoneal saline (*D* and *F*) or leptin (2 μg/g) (*E* and *G*). *H*: Quantification of c-Fos–positive cell number per brain section in WT and POMC-λKO mice treated with intraperitoneal saline (Sal) or leptin (Lep). *I*: Hypothalamic expression levels of *Pomc*, *Pcsk1*, *Pcsk2*, *Cpe*, and *Pam* mRNA. *J* and *K*: Representative images showing immunostaining of α-MSH in the PVN. *L*: Quantification of α-MSH immunoreactivity in the PVN. Bars represent the mean ± SEM of four sections from three animals per group. $^{*}P < 0.05$; $^{**}P < 0.001$; $^{***}P < 0.001$. n.s., not significant.

findings suggest that the PI3K pathway receives multiple inputs (e.g., insulin, leptin, nutrients, cytokines) but integrates them in complex ways to enable POMC neurons to influence specific physiological functions such as energy and glucose homeostasis.

As described earlier, aPKC acts as an important leptin signaling intermediate downstream of PI3K. In addition, we discovered that melanocortin content is reduced in POMC-λKO mice despite increased *Pomc* gene expression. Thus, aPKC activity in POMC neurons may have a leptin-independent role in regulating energy homeostasis, possibly through reduced expression of *Pam*. Interestingly, PAM heterozygotes have a late-onset obesity and glucose intolerance phenotype (37), consistent with a function in energy metabolism. Furthermore, amidation by PAM converts α-$MSH_{1–14}$ to des-acetyl-α-$MSH_{1–13}$, which is critical for neuropeptide stability and bioactivity (38); however, PAM also supports trafficking of secretory granules to the cell surface (39). This latter property could prevent α-MSH transport to nerve terminals, consistent with the reduced melanocortin content in the PVN of POMC-λKO mice. A reduction in PVN melanocortin

signaling would also explain the prominent hyperphagia component of the POMC-λKO phenotype, as PVN MC4R neurons regulate food intake but not energy expenditure (40,41). Future studies are needed to determine the role of aPKC in the regulation of PAM expression and to characterize the defect in melanocortin production in POMC-λKO mice.

Much like other PI3K pathway intermediates (7–9,11–14), PKC-λ functions in POMC neurons to limit susceptibility to weight gain and glucose intolerance only in mice fed an HFD. However, CNS-wide aPKC inhibition alters metabolic parameters, even on a chow diet. While the mechanism underlying this distinction remains unknown, one hypothesis supported by this study is that regulation of energy homeostasis by aPKC action occurs in diverse neuronal populations that only include POMC neurons with a higher level of aPKC expression during DIO (perhaps because of the hyperleptinemia and hyperinsulinemia associated with HFD feeding [26]). Future experiments involving targeted overexpression of aPKC in POMC neurons and deletion of aPKC from other key neurons involved in energy homeostasis regulation should help resolve this unanswered question.

A common feature of mouse models with altered signaling in POMC neurons is the generally more profound disruption of glucose homeostasis than energy balance. In leptin receptor–deficient mice in which leptin signaling has been restored exclusively in POMC neurons, amelioration of the obese phenotype is modest, yet insulin sensitivity returns to WT levels (42,43). Likewise, deletion of the leptin receptor from POMC neurons disrupts glucose homeostasis but does not affect leptin-mediated anorexia (44). In addition, a variety of POMC neuron–specific KOs have exclusively glucose-related phenotypes (Lkb1 [45], GLP2 [46], S6K [47]). We observed a similarly profound disruption of both glucose tolerance and insulin sensitivity in POMC-λKO mice that was detectable at low levels even within 1 week of HFD feeding in relatively lean mice. This effect was magnified by the increased adiposity of POMC-λKO mice during prolonged DIO. Nevertheless, its presence before weight gain and the acute worsening of glucose tolerance observed with INH treatment are consistent with a weight-independent effect on glucose homeostasis. Because central infusion of leptin improves glucose tolerance via a PI3K-dependent pathway (48–50), aPKC inhibition may exert its glucoregulatory effects through impairment of leptin signaling. Nevertheless, both POMC aPKC deletion and CNS aPKC inhibition cause only modest, weight-independent glucose intolerance, suggesting that the primary effect of disrupting CNS aPKC is to amplify the deleterious effects of HFD feeding and weight gain on glucose homeostasis.

An interesting but unresolved issue is the high frequency of sex-specific metabolic phenotypes in mouse models with altered leptin signaling. Leptin-deficient *ob/ob* mice have sex-specific metabolomics profiles (51), and alteration of the leptin receptor Y985 residue enhances leptin sensitivity and prevents DIO only in female mice (52). Similarly, female rodents are more sensitive to the anorexic effects of leptin infusion, whereas males respond more robustly to insulin (53). Deletion of the leptin receptor alone (8) or in combination with the insulin receptor (35), the phosphatidylinositol (3,4,5)-trisphosphate phosphatase Pten (54), the AMPK-regulating kinase Lkb1 (45), and the leptin signaling transcription factor Stat3 (10) all cause obesity in a sex-specific manner. POMC-λKO mice also show sexual dimorphism in their metabolic phenotype: only males have enhanced susceptibility to DIO and disrupted glucose homeostasis. Because neither sex-specific regulation of aPKC expression and function nor altered fertility was observed in POMC-λKO mice (M.D.D. and J.P.T., unpublished observations), the mechanism underlying the sex differences remains unknown. Though more studies are needed, the female-specific anorexigenic action of estrogen in POMC neurons (55) may contribute to this dimorphism by disproportionately protecting females from obesity-inducing diets and genetic insults.

Previous work on neuronal aPKC has been limited by the fact that pan-neuronal PKC-λKOs die during embryogenesis because of defects in cortical neuroepithelial development (24). Similarly, overexpression of PKC-λ or deletion of the truncated constitutively active PKC-ζ isoform PKM-ζ disrupts hippocampal neurogenesis (25). In this study, however, deletion of PKC-λ did not affect the number or localization of POMC neurons within the hypothalamus. In addition, the INH studies demonstrate a postnatal metabolic effect of CNS aPKC inhibition that cannot be explained by developmental compensation. It should be noted that although the specificity of INH has been recently questioned (56,57), INH demonstrably disrupts a critical interaction between aPKC and the cytoplasmic regulator p62/Sequestosome1 (58), an important mediator of aPKC action. Strikingly, p62 is highly expressed in POMC neurons, and the p62-deficient mouse shows resistance to leptin, hyperphagia, and obesity (59). Future work is necessary to establish whether p62 is a bona fide aPKC target in the hypothalamus.

Our study focused on the metabolic phenotype resulting from deletion of aPKC from arcuate POMC neurons. However, nonarcuate sites of aPKC action may also contribute to the alterations in energy homeostasis observed in this model. Indeed, gene deletion using the *Pomc-Cre* transgene occurs outside of arcuate POMC neurons, including in nonhypothalamic POMC cell populations such as pituitary corticotrophs, hindbrain nucleus tractus solitarius (NTS) neurons, and a subset of arcuate NPY/AgRP neurons that transiently express POMC during development (60,61). While we cannot exclude a contribution of NPY/AgRP aPKC to the POMC-λKO phenotype, action in pituitary or NTS cells is less likely. Corticotroph function is preserved in POMC-λKO mice, with a diet-independent increase rather than decrease in corticosterone secretion (Supplementary Fig. 3). In addition, the

elevated corticosterone levels in female POMC-λKO mice without a discernible metabolic phenotype suggest that susceptibility to DIO is unrelated to glucocorticoid action. Interestingly, this contrasts with other POMC-specific KO models such as the POMC Pdk1-deficient mouse that suffers hypocortisolism as a result of impaired corticotroph function and requires cortisol replacement to manifest obesity (13,14). The NTS POMC neuron population is poorly understood, but ablation studies have demonstrated a contribution to only acute feeding behavior, not chronic energy balance regulation or obesity (42,62,63). In addition, hindbrain POMC neurons do not seem to be regulated by leptin (64,65). In the POMC-λKO model, acute feeding parameters were generally unchanged; only a chronic excess of HFD intake eventually resulted in increased susceptibility to DIO through reduced sensitivity to leptin. Future studies with targeted inhibition or viral knockdown of aPKC will help clarify whether additional sites of aPKC action contribute to energy and glucose homeostasis.

In summary, we found that the PI3K effector enzyme aPKC is regulated in the hypothalamus by leptin and HFD feeding. Either pharmacological disruption of aPKC activity throughout the CNS or genetic deletion of the aPKC isoform PKC-λ in POMC neurons causes increased susceptibility to HFD-induced obesity, hyperphagia, and glucose intolerance. In contrast with the detrimental impact of hepatic aPKC action (19,20), the protective function of CNS aPKC highlights the complexities of using chemical aPKC inhibitors in the treatment of obesity and diabetes (66), and provides a mechanistic basis to develop CNS-sparing agents to ensure their metabolic efficacy.

Acknowledgments. The authors acknowledge the technical assistance provided by Rachael Fasnacht, Lee Shaffer, Alex Cubelo, J.D. Fisher, and Loan Nguyen at the University of Washington, and many discussions with Thomas H. Meek and other members of the M.W. Schwartz Laboratory. The authors are also grateful to Dr. Gregory Barsh (Stanford University) for providing the *Pomc-Cre* mice, and to Dr. Tamas Horvath (Yale University) for the *Pomc-Tau-Gfp* mice.

Funding. This work was supported by a mentor-based postdoctoral fellowship from the American Diabetes Association (ADA) (grant 7-11-MN-49 to M.D.D.), by the National Institutes of Health (NIH) (grant DK089056 to G.J.M. and grant DK052989 to M.W.S.), and by the ADA Pathway to Stop Diabetes (grant 1-14-ACE-51), the University of Washington Royalty Research Fund Award, and a National Institute of Diabetes and Digestive and Kidney Diseases Career Development Award (DK088872) to J.P.T. Services and support were provided by the Nutrition Obesity Research Center (DK035816) and Diabetes Research Center (DK017047) at the University of Washington.

Duality of Interest. No potential conflicts of interest relevant to this article were reported.

Author Contributions. M.D.D. and J.P.T. designed the overall study, analyzed all data, and wrote the manuscript. M.D.D., J.E.K., J.M.S., and S.J.G. performed experiments and collected data. M.P.S. and R.V.F. provided aPKC activity data. V.D. and H.T.N. helped perform initial pilot studies. M.L. provided reagents. G.J.M., R.V.F., and M.W.S. designed experiments, provided conceptual advice, and edited the manuscript. M.W.S. supervised the initial pilot studies. J.P.T. performed the initial pilot studies. J.P.T. is the guarantor of this work and, as such, had full access to all the data in the study and takes responsibility for the integrity of the data and the accuracy of the data analysis.

References

1. Schwartz MW, Woods SC, Porte D Jr, Seeley RJ, Baskin DG. Central nervous system control of food intake. Nature 2000;404:661–671

2. Garfield AS, Lam DD, Marston OJ, Przydzial MJ, Heisler LK. Role of central melanocortin pathways in energy homeostasis. Trends Endocrinol Metab 2009; 20:203–215

3. Mountjoy KG. Pro-opiomelanocortin (POMC) neurones, POMC-derived peptides, melanocortin receptors and obesity: how understanding of this system has changed over the last decade. J Neuroendocrinol 2015;27:406–418

4. Varela L, Horvath TL. Leptin and insulin pathways in POMC and AgRP neurons that modulate energy balance and glucose homeostasis. EMBO Rep 2012;13:1079–1086

5. Qiu J, Fang Y, Rønnekleiv OK, Kelly MJ. Leptin excites proopiomelanocortin neurons via activation of TRPC channels. J Neurosci 2010;30:1560–1565

6. Morton GJ, Cummings DE, Baskin DG, Barsh GS, Schwartz MW. Central nervous system control of food intake and body weight. Nature 2006;443:289–295

7. Balthasar N, Coppari R, McMinn J, et al. Leptin receptor signaling in POMC neurons is required for normal body weight homeostasis. Neuron 2004;42:983–991

8. Shi H, Strader AD, Sorrell JE, Chambers JB, Woods SC, Seeley RJ. Sexually different actions of leptin in proopiomelanocortin neurons to regulate glucose homeostasis. Am J Physiol Endocrinol Metab 2008;294:E630–E639

9. van de Wall E, Leshan R, Xu AW, et al. Collective and individual functions of leptin receptor modulated neurons controlling metabolism and ingestion. Endocrinology 2008;149:1773–1785

10. Xu AW, Ste-Marie L, Kaelin CB, Barsh GS. Inactivation of signal transducer and activator of transcription 3 in proopiomelanocortin (Pomc) neurons causes decreased Pomc expression, mild obesity, and defects in compensatory refeeding. Endocrinology 2007;148:72–80

11. Al-Qassab H, Smith MA, Irvine EE, et al. Dominant role of the p110beta isoform of PI3K over p110alpha in energy homeostasis regulation by POMC and AgRP neurons. Cell Metab 2009;10:343–354

12. Hill JW, Xu Y, Preitner F, et al. Phosphatidyl inositol 3-kinase signaling in hypothalamic proopiomelanocortin neurons contributes to the regulation of glucose homeostasis. Endocrinology 2009;150:4874–4882

13. Belgardt BF, Husch A, Rother E, et al. PDK1 deficiency in POMC-expressing cells reveals FOXO1-dependent and -independent pathways in control of energy homeostasis and stress response. Cell Metab 2008;7:291–301

14. Iskandar K, Cao Y, Hayashi Y, et al. PDK-1/FoxO1 pathway in POMC neurons regulates Pomc expression and food intake. Am J Physiol Endocrinol Metab 2010;298:E787–E798

15. Bandyopadhyay G, Standaert ML, Galloway L, Moscat J, Farese RV. Evidence for involvement of protein kinase C (PKC)-zeta and noninvolvement of diacylglycerol-sensitive PKCs in insulin-stimulated glucose transport in L6 myotubes. Endocrinology 1997;138:4721–4731

16. Standaert ML, Galloway L, Karnam P, Bandyopadhyay G, Moscat J, Farese RV. Protein kinase C-zeta as a downstream effector of phosphatidylinositol 3-kinase during insulin stimulation in rat adipocytes. Potential role in glucose transport. J Biol Chem 1997;272:30075–30082

17. Seidl S, Braun U, Roos N, et al. Phenotypical analysis of atypical PKCs in vivo function display a compensatory system at mouse embryonic day 7.5. PLoS One 2013;8:e62756

18. Farese RV, Sajan MP, Yang H, et al. Muscle-specific knockout of PKC-lambda impairs glucose transport and induces metabolic and diabetic syndromes. J Clin Invest 2007;117:2289–2301

19. Habegger KM, Matzke D, Ottaway N, et al. Role of adipose and hepatic atypical protein kinase C lambda (PKCλ) in the development of obesity and glucose intolerance. Adipocyte 2012;1:203–214
20. Sajan MP, Ivey RA, Lee MC, Farese RV. Hepatic insulin resistance in ob/ob mice involves increases in ceramide, aPKC activity, and selective impairment of Akt-dependent FoxO1 phosphorylation. J Lipid Res 2015;56:70–80
21. Sajan MP, Ivey RA 3rd, Lee M, et al. PKCλ haploinsufficiency prevents diabetes by a mechanism involving alterations in hepatic enzymes. Mol Endocrinol 2014;28:1097–1107
22. Lee SJ, Kim JY, Nogueiras R, et al. PKCzeta-regulated inflammation in the nonhematopoietic compartment is critical for obesity-induced glucose intolerance. Cell Metab 2010;12:65–77
23. Oster H, Eichele G, Leitges M. Differential expression of atypical PKCs in the adult mouse brain. Brain Res Mol Brain Res 2004;127:79–88
24. Imai F, Hirai S, Akimoto K, et al. Inactivation of aPKClambda results in the loss of adherens junctions in neuroepithelial cells without affecting neurogenesis in mouse neocortex. Development 2006;133:1735–1744
25. Parker SS, Mandell EK, Hapak SM, et al. Competing molecular interactions of aPKC isoforms regulate neuronal polarity. Proc Natl Acad Sci U S A 2013;110:14450–14455
26. Thaler JP, Choi SJ, Sajan MP, et al. Atypical protein kinase C activity in the hypothalamus is required for lipopolysaccharide-mediated sickness responses. Endocrinology 2009;150:5362–5372
27. Eichholtz T, de Bont DB, de Widt J, Liskamp RM, Ploegh HL. A myristoylated pseudosubstrate peptide, a novel protein kinase C inhibitor. J Biol Chem 1993;268:1982–1986
28. Bandyopadhyay G, Standaert ML, Sajan MP, et al. Protein kinase C-lambda knockout in embryonic stem cells and adipocytes impairs insulin-stimulated glucose transport. Mol Endocrinol 2004;18:373–383
29. Sengupta A, Duran A, Ishikawa E, et al. Atypical protein kinase C (aPKCzeta and aPKClambda) is dispensable for mammalian hematopoietic stem cell activity and blood formation. Proc Natl Acad Sci U S A 2011;108:9957–9962
30. Matsen ME, Thaler JP, Wisse BE, et al. In uncontrolled diabetes, thyroid hormone and sympathetic activators induce thermogenesis without increasing glucose uptake in brown adipose tissue. Am J Physiol Endocrinol Metab 2013;304:E734–E746
31. Taicher GZ, Tinsley FC, Reiderman A, Heiman ML. Quantitative magnetic resonance (QMR) method for bone and whole-body-composition analysis. Anal Bioanal Chem 2003;377:990–1002
32. Scarlett JM, Jobst EE, Enriori PJ, et al. Regulation of central melanocortin signaling by interleukin-1 beta. Endocrinology 2007;148:4217–4225
33. Wardlaw SL. Hypothalamic proopiomelanocortin processing and the regulation of energy balance. Eur J Pharmacol 2011;660:213–219
34. Williams KW, Margatho LO, Lee CE, et al. Segregation of acute leptin and insulin effects in distinct populations of arcuate proopiomelanocortin neurons. J Neurosci 2010;30:2472–2479
35. Hill JW, Elias CF, Fukuda M, et al. Direct insulin and leptin action on pro-opiomelanocortin neurons is required for normal glucose homeostasis and fertility. Cell Metab 2010;11:286–297
36. Faulkner LD, Dowling AR, Stuart RC, Nillni EA, Hill JW. Reduced melanocortin production causes sexual dysfunction in male mice with POMC neuronal insulin and leptin insensitivity. Endocrinology 2015;156:1372–1385
37. Czyzyk TA, Ning Y, Hsu MS, et al. Deletion of peptide amidation enzymatic activity leads to edema and embryonic lethality in the mouse. Dev Biol 2005;287:301–313
38. Pritchard LE, Turnbull AV, White A. Pro-opiomelanocortin processing in the hypothalamus: impact on melanocortin signalling and obesity. J Endocrinol 2002;172:411–421
39. Ciccotosto GD, Schiller MR, Eipper BA, Mains RE. Induction of integral membrane PAM expression in AtT-20 cells alters the storage and trafficking of POMC and PC1. J Cell Biol 1999;144:459–471
40. Balthasar N, Dalgaard LT, Lee CE, et al. Divergence of melanocortin pathways in the control of food intake and energy expenditure. Cell 2005;123:493–505
41. Krashes MJ, Lowell BB, Garfield AS. Melanocortin-4 receptor-regulated energy homeostasis. Nat Neurosci 2016;19:206–219
42. Berglund ED, Vianna CR, Donato J Jr, et al. Direct leptin action on POMC neurons regulates glucose homeostasis and hepatic insulin sensitivity in mice. J Clin Invest 2012;122:1000–1009
43. Huo L, Gamber K, Greeley S, et al. Leptin-dependent control of glucose balance and locomotor activity by POMC neurons. Cell Metab 2009;9:537–547
44. do Carmo JM, da Silva AA, Wang Z, et al. Regulation of blood pressure, appetite, and glucose by leptin after inactivation of insulin receptor substrate 2 signaling in the entire brain or in proopiomelanocortin neurons. Hypertension 2016;67:378–386
45. Claret M, Smith MA, Knauf C, et al. Deletion of Lkb1 in pro-opiomelanocortin neurons impairs peripheral glucose homeostasis in mice. Diabetes 2011;60:735–745
46. Shi X, Zhou F, Li X, et al. Central GLP-2 enhances hepatic insulin sensitivity via activating PI3K signaling in POMC neurons. Cell Metab 2013;18:86–98
47. Smith MA, Katsouri L, Irvine EE, et al. Ribosomal S6K1 in POMC and AgRP Neurons regulates glucose homeostasis but not feeding behavior in mice. Cell Rep 2015;11:335–343
48. Obici S, Zhang BB, Karkanias G, Rossetti L. Hypothalamic insulin signaling is required for inhibition of glucose production. Nat Med 2002;8:1376–1382
49. Pocai A, Lam TK, Gutierrez-Juarez R, et al. Hypothalamic K(ATP) channels control hepatic glucose production. Nature 2005;434:1026–1031
50. Pocai A, Morgan K, Buettner C, Gutierrez-Juarez R, Obici S, Rossetti L. Central leptin acutely reverses diet-induced hepatic insulin resistance. Diabetes 2005;54:3182–3189
51. Won EY, Yoon MK, Kim SW, et al. Gender-specific metabolomic profiling of obesity in leptin-deficient ob/ob mice by ^{1}H NMR spectroscopy. PLoS One 2013;8:e75998
52. Björnholm M, Münzberg H, Leshan RL, et al. Mice lacking inhibitory leptin receptor signals are lean with normal endocrine function. J Clin Invest 2007;117:1354–1360
53. Shi H, Seeley RJ, Clegg DJ. Sexual differences in the control of energy homeostasis. Front Neuroendocrinol 2009;30:396–404
54. Plum L, Ma X, Hampel B, et al. Enhanced PIP3 signaling in POMC neurons causes KATP channel activation and leads to diet-sensitive obesity. J Clin Invest 2006;116:1886–1901
55. Xu Y, Nedungadi TP, Zhu L, et al. Distinct hypothalamic neurons mediate estrogenic effects on energy homeostasis and reproduction. Cell Metab 2011;14:453–465
56. Lee AM, Kanter BR, Wang D, et al. Prkcz null mice show normal learning and memory. Nature 2013;493:416–419
57. Bogard AS, Tavalin SJ. Protein kinase C (PKC)ζ pseudosubstrate inhibitor peptide promiscuously binds PKC family isoforms and disrupts conventional PKC targeting and translocation. Mol Pharmacol 2015;88:728–735
58. Tsai LC, Xie L, Dore K, et al. Zeta inhibitory peptide disrupts electrostatic interactions that maintain atypical protein kinase C in its active conformation on the scaffold p62. J Biol Chem 2015;290:21845–21856
59. Harada H, Warabi E, Matsuki T, et al. Deficiency of p62/Sequestosome 1 causes hyperphagia due to leptin resistance in the brain. J Neurosci 2013;33:14767–14777
60. Padilla SL, Reef D, Zeltser LM. Defining POMC neurons using transgenic reagents: impact of transient Pomc expression in diverse immature neuronal populations. Endocrinology 2012;153:1219–1231

61. Padilla SL, Carmody JS, Zeltser LM. Pomc-expressing progenitors give rise to antagonistic neuronal populations in hypothalamic feeding circuits. Nat Med 2010;16:403–405
62. Lam DD, Attard CA, Mercer AJ, Myers MG Jr, Rubinstein M, Low MJ. Conditional expression of Pomc in the Lepr-positive subpopulation of POMC neurons is sufficient for normal energy homeostasis and metabolism. Endocrinology 2015;156:1292–1302
63. Zhan C, Zhou J, Feng Q, et al. Acute and long-term suppression of feeding behavior by POMC neurons in the brainstem and hypothalamus, respectively. J Neurosci 2013;33:3624–3632
64. Garfield AS, Patterson C, Skora S, et al. Neurochemical characterization of body weight-regulating leptin receptor neurons in the nucleus of the solitary tract. Endocrinology 2012;153:4600–4607
65. Huo L, Grill HJ, Bjørbaek C. Divergent regulation of proopiomelanocortin neurons by leptin in the nucleus of the solitary tract and in the arcuate hypothalamic nucleus. Diabetes 2006;55:567–573
66. Farese RV, Lee MC, Sajan MP. Atypical PKC: a target for treating insulin-resistant disorders of obesity, the metabolic syndrome and type 2 diabetes mellitus. Expert Opin Ther Targets 2014;18:1163–1175